Experimental evidence for logarithmic fractal structure of botanical trees

S. V. Grigoriev [1,2] O. D. Shnyrkov [1] P. M. Pustovoit,[1] E. G. Iashina [1,2] and K. A. Pshenichnyi[1]

[1]*Petersburg Nuclear Physics Institute, NRC "Kurchatov Institute," Orlova Roscha, Gatchina 188300, Russia*
[2]*Saint Petersburg State University, Ulyanovskaya 1, Saint Petersburg 198504, Russia*

The area-preserving rule for botanical trees by Leonardo da Vinci is discussed in terms of a very specific fractal structure, a logarithmic fractal. We use a method of the numerical Fourier analysis to distinguish the logarithmic fractal properties of the two-dimensional objects and apply it to study the branching system of real trees through its projection on the two-dimensional space, i.e., using their photographs. For different species of trees (birch and oak) we observe the Q^{-2} decay of the spectral intensity characterizing the branching structure that is associated with the logarithmic fractal structure in two-dimensional space. The experiments dealing with the side view of the tree should complement the area preserving Leonardo's rule with one applying to the product of diameter d and length l of the k branches: $d_i\, l_i = k\, d_{i+1}\, l_{i+1}$. If both rules are valid, then the branch's length of the next generation is $\sqrt{k}$ times shorter than previous one: $l_i = \sqrt{k}\, l_{i+1}$. Moreover, the volume (mass) of all branches of the next generation is a factor of d_i/d_{i+1} smaller than previous one. We conclude that a tree as a three-dimensional object is not a logarithmic fractal, although its projection onto a two-dimensional plane is. Consequently, the life of a tree flows according to the laws of conservation of area in two-dimensional space, as if the tree were a two-dimensional object.

I. INTRODUCTION

One of the discoveries of Leonardo da Vinci is known as the area-preserving rule that the section area below a given branching point is equal to the sum of the section areas of the daughter branches above this point: $d_i^2 = k\, d_{i+1}^2$ with d the diameter of the branch and k the number of branches [1]. This formulation underlies the structural properties of tree models [2–9] and builds a playground for computer modeling of treelike objects [10,11]. Although Leonardo's rule is widely used in theoretical models, computer modeling, and allometric studies [4–8], there is very little experimental work confirming its validity. Moreover, the authors of the extended and deep review [9] analyzing available experimental works [12–14] have concluded that "the Leonardo da Vinci's rule does not hold in general conditions." Indeed, the experimental proof of this law requires great physical efforts and dexterity from the experimenter, if he or she decides to measure each branch of the tree without harming the tree itself.

In this paper we propose and test experimentally a way (accessible to everyone) to convince oneself that a branching system of a typical tree is described by a special, logarithmic fractal structure obeying the area-preserving (*Leonardo-like*) rule. We believe that we give experts a tool with which to measure the beauty of a tree through the fractal characteristics, such as the logarithmic subdimension and an applicable scaling range. We start with the famous book of Mandelbrot [15], where he not only gave the general definition of the fractal objects but also described the borderline case, the so-called logarithmic fractal. Its probing function for the fractal measure can be written for the ruler length r as

$$h(r) = r^{D_f}[\ln(1/r)]^{\Delta}, \qquad (1)$$

where $D_f = D_T$ (D_T is a topological dimension) and Δ is a subdimension.

These logarithmic fractals have received minimal, if not zero, attention for the simple reason that no one has understood how many objects with the logarithmic fractal structure surround us. The botanical tree branching structure is a prime example of the logarithmic fractal that was first noticed in [16]. Indekeu *et al.* presented the top-bottom view of the sections of several successive levels of a branching tree constructed according to Leonardo's rule (see the inset in Fig. 1). It was shown that the top-bottom view of the tree is the logarithmic fractal since this image is described by the probing function given by Eq. (1) with $D_f = 2$ and $\Delta = -1$ [16]. In other words, the logarithmic fractal with $D_f = 2$ and $\Delta = -1$ is an adequate mathematical model for description of the top-bottom view of the tree built on Leonardo's principle. The equivalence of Leonardo's principle and the logarithmic fractal structure is shown in Appendix A.

Logarithmic fractals have features distinguishing them from the classical fractals. First, the area of a logarithmic fractal, in contrast to the classical one, increases with an additive rather than multiplicative constant, upon reducing the ruler length by a fixed rescaling factor. This property reflects directly the area-preserving Leonardo's rule. Second, the logarithmic fractal is self-similar but not uniform. The object can be "dated" locally since the size of its sections is indicative of their age [16].

Leonardo's own sketches demonstrate the side (not top-bottom) views of the tree [1], as the primary goal of the artist was to reflect the beauty of the tree as seen by human eyes. A model for the side view, often referred as a Pythagoras tree [17], is built on the Pythagorean theorem: the three sides of a
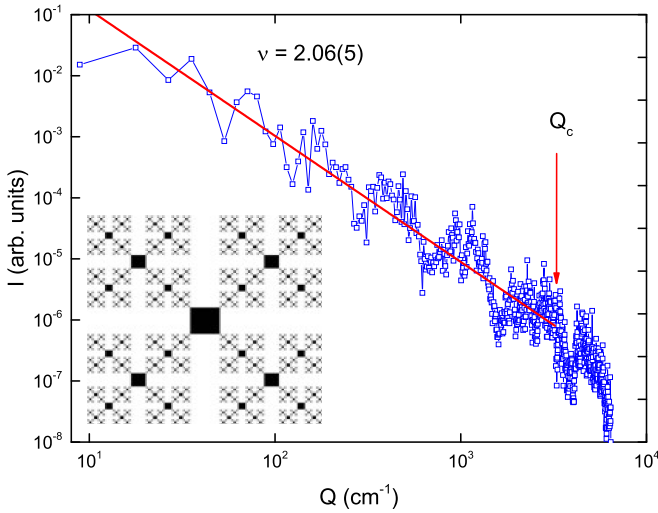
FIG. 1. The averaged intensities vs Fourier coordinate Q for the picture of the seventh generation of the Leonardo tree (top-bottom view). The latter is shown as inset.

right triangle are interconnected so that the area of the square built on the hypotenuse is equal to the sum of squares' areas of its legs (see an inset in Fig. 2). The principle of a Pythagoras tree obeys the area-preserving rule, similarly to Leonardo's rule. The insignificant difference in the two principles is that the Pythagoras tree splits for two branches only at each generation, while the number of branches is not limited for the Leonardo tree. It is interesting to note that the Pythagoras tree (inset in Fig. 2) can be disposed into three Leonardo trees (inset in Fig. 1): one is composed of the first, third, fifth, etc. generations, while the other two are made of the second, fourth, sixth, etc. generations. Therefore the Pythagoras tree can be identified as the logarithmic fractal with the fractal measure given by Eq. (1) and the same $D_f = 2$ and $\Delta = -1$ (as well as the Leonardo tree). Using this scaling properties
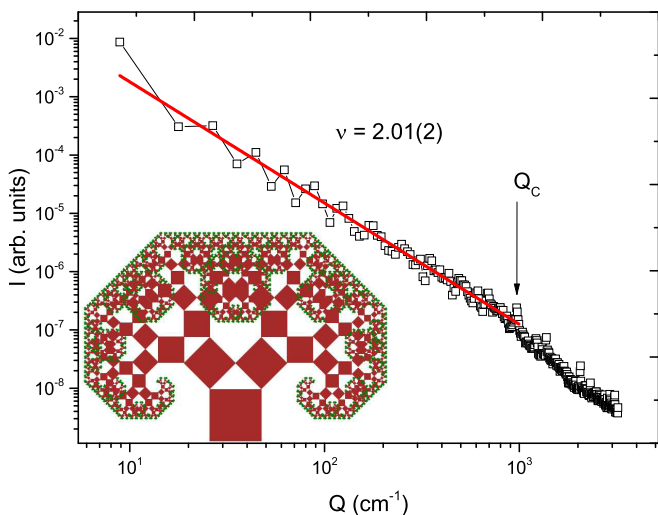

FIG. 2. The averaged intensities vs Fourier coordinate Q for the picture of the eleventh generation of the Pythagoras tree (side view). The latter is shown as inset.

one can theoretically prove that the "forest" modeled from the Leonardo trees is one very big *tree* that is described as the logarithmic fractal. Please note that this concept supports the theory of the forest taken as "a scaled version of the branching network of the largest tree" [6].

There have been numerous attempts to construct tree models based on the physical properties of real botanical trees [2,3,9,10]. Both the "pipe model" [2,9] and the elastic similarity model [3] rely on the scaling properties of the branching tree referring to their fractal nature. In an attempt to modernize the elastic similarity model the author of [10] suggested distinguishing the fractal properties of the branch's diameter obeying Leonardo's rule and that of a branch's length described by the classical fractal structure, thus pointing out the importance of accounting for the branch's length. However, the understanding that Leonardo's rule is equivalent to the logarithmic fractal structure was still missing. Equally mistakenly, without any experimental evidence it was stated that the branch length obeys the law of the classical fractal.

In this paper, in Sec. II we introduce the numerical Fourier analysis as an analog of the small angle scattering (SAS) technique that has its own classification of fractal objects and that distinguishes cases of volume fractals and surface fractals. Moreover, SAS techniques are able to identify an intermediate case, logarithmic fractals. In Sec. III we apply numerical Fourier analysis as an analog of SAS to the pictures of the Leonardo tree and Pythagoras tree and demonstrate that these objects can be considered and called logarithmic fractals. These numerical experiments support the theoretical consideration given in [16]. In Sec. IV we apply the numerical Fourier analysis to the photos of trees and find that it obeys the same law (ν close to 2) that is identified as a signature of the logarithmic fractal structure of the object and therefore establish an area-preserving rule, now for the side view of the real trees. This approach shows that it is the branching mechanism that seems to impose solid restrictions on both diameter and length of the tree branches resulting in the logarithmic fractal scaling of both parameters. Further on, the numerical experiments dealing with the side view of the tree complement the area-preserving Leonardo's rule with one applying to the product of diameter d and length l of the branches: $d_i l_i = k d_{i+1} l_{i+1}$. In conclusion, in Sec. V we state that the life of a tree flows according to the laws of conservation of area in two-dimensional space, as if the tree were a two-dimensional object. The paper is supplemented by two Appendixes.

II. CLASSIFICATION OF FRACTALS BY SAS

Unlike mathematical and geometrical fractals, the physical fractals require the instruments to verify their fractal properties and to directly measure its fractal dimension. One of the direct methods to study fractals on the scales of nano- and microworlds is small-angle scattering of neutrons or x-rays [18–24]. The scattering intensity $I(Q)$ is related to inhomogeneities of the scattering density $\rho(r)$ and is equal to the Fourier transform of the correlation function of the object $\gamma(r)$. The self-similarity of an unlimited in size fractal object is converted to the power law of scattering intensity as a

function of momentum transfer $I(Q) \sim Q^{-\nu}$ [23,24]. For the objects of the finite size ξ, the scattering intensity can be given in a more general way as

$$I(Q) \sim \frac{1}{[1 + (Q\xi)^2]^{\nu/2}}, \qquad (2)$$

where ν is an exponent associated with the fractal dimension. Moreover, the SAS method introduces the classification of fractal objects through the value of the exponent ν [23–25]. It identifies scattering on three-dimensional nonfractal particles as being well described by Eq. (2) with $\nu = 4$. The deviation of ν from 4 indicates the fractal structure of the particle: $4 > \nu > 3$ for the surface fractal and $3 > \nu > 2$ for the mass fractal. The intermediate case with $\nu = 3$ between the mass and the surface fractals is identified as a special class of the logarithmic fractals [25].

The methodology of SAS can also be applied to fractal objects, such as a Leonardo tree or Pythagoras tree. In this case, first, we deal with objects in the two-dimensional space and, second, we can treat fractal images using a numerical Fourier transformation. The scheme of a numerical Fourier analysis of an object in a two-dimensional space consists of the following four steps. The object under study is a square image, described by a binary two-dimensional matrix. The first step is to perform a Fourier transform of the object. The resulting Fourier image will also be a two-dimensional matrix with each element characterized by an amplitude and a phase. The second step is the formation of a two-dimensional map as the square of the Fourier image, which simulates the intensity of SAS. At this step, the phase of the Fourier image is lost. The third step of the scheme is the azimuth averaging of the intensity map around the center and obtaining a curve of the averaged intensity, analog of a SAS curve, i.e., dependence of the scattering intensity on the momentum transfer $I(Q)$ [Eq. (2)]. The last step is to determine of the exponent ν as the ratio of the logarithms of the averaged intensity $\ln(I)$ and the Fourier coordinate $\ln(Q)$. The exponent ν is directly related to the fractal dimension D, but in different ways for three-dimensional space (SAS case) and for two-dimensional space (Fourier images of trees).

The loss of one spatial dimension leads to a decrease in all numbers of the fractal classification by one. For homogeneously filled (nonfractal) objects with a sharp boundary (a filled circle, for example), the scattering intensity decreases with Q obeying Eq. (2) with $\nu = 3$. The fractal objects in the two-dimensional space (in analogy with ones in three-dimensional space) are classified and split onto two classes of the "mass" and "boundary" fractals. Thus, for the "mass" fractals ν lays within the limits $1 < \nu < 2$. For the "boundary" fractals the exponent ν lies in the range $2 < \nu < 3$. Again the margin case with $\nu = 2$ describes the logarithmic fractal structure. The classification of fractal objects in two-dimensional space is given in [26].

III. FOURIER ANALYSIS OF THEE MODELS

To show the possibilities opened by Fourier analysis to quantitatively characterize fractal objects in two-dimensional space, we performed the numerical experiments [27] for the

Leonardo tree of the seventh generation (Fig. 1) and for the Pythagoras tree of the eleventh generation (Fig. 2). The slope of the curves presented in log-log scales appeared to be equal to $\nu = 2.06 \pm 0.05$ for the Leonardo tree and $\nu = 2.01 \pm 0.02$ for the Pythagoras tree. The curve for the Leonardo tree (Fig. 1) demonstrates the oscillating behavior imposed on a Q^{-2} decay toward increase of momentum transfer Q. The oscillations are caused by the regular structure of the object. They have a quasiperiodic character on the logarithmic scale in the left side of the curves that points to the fractal properties of the object under study. The decaying exponent (slope of the curves in the log-log scales) changes upon increase of momentum transfer Q. The crossover point between two regimes (denoted as Q_c in Figs. 1 and 2) characterizes the small-scale fractal border, i.e., the linear size of the minimal element of the fractal.

It is shown in Appendix B that the correlation function γ of the object in the two-dimensional space whose scattering cross section is described by Eq. (2) with $\nu = 2$ is proportional to $\ln(\xi/r)$ in the approximation of $r/\xi < 1$, i.e., inside the fractal particle of a size ξ. Thus, the correlation function of the logarithmic fractal is related to the probing function h [Eq. (1)] as they characterize the very same fractal object. In accord with the derivations given in Appendix A and Appendix B, $h(r) \sim r^2[\gamma(r)]^{-1}$.

The theoretical models (the Leonardo tree and Pythagorean tree) are both shown to have the properties of the logarithmic fractal and as such are a good starting point for the real tree modeling. These both models have deal with the area-preserving principles: $d_i^2 = k\, d_{i+1}^2$ for the Leonardo tree and $d_i l_i = 2\, d_{i+1} l_{i+1}$ for the Pythagorean tree, where d_i is the thickness of a branch and l_i is the length of a branch of ith generation. Note that $d_i = l_i$ for the Pythagorean tree (see inset of Fig. 2). For the real trees $d_i \ll l_i$, and if one elongates one side of its each element by the same factor, say, 3, then the area-preserving rule is still fulfilled, while the image of such a tree becomes much closer to real tree photos. This object again can be characterized by the probing function of the logarithmic fractal given by Eq. (1). The Fourier analysis for the modified Pythagoras tree of the seventh generation gives the slope of the curve in the log-log scale close to 2. Thus, the logarithmic fractals tested using Fourier analysis (SAS methodology) follow a power law [Eq. (2)] with ν close or equal to 2.

To make further steps in the real tree modeling one has to set, first, the branching number k arbitrary, but, second, to address the question if both area-preserving principles can be fulfilled simultaneously. In other words, we have to combine the pictures of the Leonardo tree and the Pythagoras tree as two-dimensional images into one three-dimensional object. The supposition that Leonardo's rule is valid results in the restriction imposed on the branch's length: the next generation is $\sqrt{k}$ times shorter than the previous one: $l_i = \sqrt{k}\, l_{i+1}$. Moreover, our rule leads to the formulation on the volume (mass) of different branching levels: the volume of all daughter branches is a factor of d_i/d_{i+1} smaller than a mother branch. It is important to note that as the volume of the different branching levels changes, then the tree as a three-dimensional object is *not* the logarithmic fractal, although its projections on the two-dimensional planes are.

FIG. 3. The photo image of a real birch used for the numerical experiment.

IV. FOURIER ANALYSIS FOR REAL TREES

Using the above described methodology we can show experimentally that any deciduous tree has the logarithmic fractal structure for its branching system. For example, one takes a photo of the tree in a winter season ensuring that leaves do not obscure its branching structure. Furthermore, using the same procedure as was applied to the Leonardo and Pythagoras trees, one examines images of real trees (birch, oak, maple, and/or any others). Photos of real birch and oak trees are shown in Figs. 3 and Fig. 5. The available images represent a projection of a real tree onto a two-dimensional plane.

FIG. 4. Fourier intensity of the birch image as a function of the Fourier coordinate Q. The inset shows the Kratky plot IQ^2 as a function of Q.

FIG. 5. Photo image of a real oak used for the numerical experiment.

These images were investigated with the Fourier analysis method.

The squared Fourier transformation of the birch's image with its consequent azimuthal averaging results in the Q dependence of the intensity $[I(Q)]$ and is presented in Fig. 4. Plotted in the log-log scales, it demonstrates clearly three Q ranges with different slopes separated by the crossovers which are pointed to by two arrows. The Q range on the left (smallest Q) characterizes the Fourier image of a homogeneous object with sharp boundaries with a slope ν close to 3. This is a computational artifact that comes from the fact that the background of the image is not 100% white, but actually gray. The Q range in the middle (between two arrows) corresponds to the net of branches from the smallest (of order of 10 cm) to the largest (of order of meters). The Q dependence of intensity $I(q)$ demonstrates a power law (2) with $\nu = 1.99 \pm 0.03$. This slope evidences the logarithmic fractal structure of the tree branching system. The scaling element is a part of branch between two branching points characterized by the width d_i and length l_i of the ith generation.
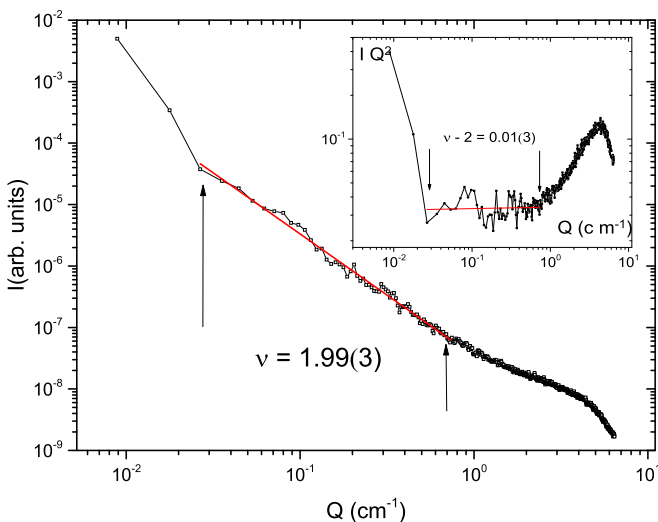
To see better and to clearly distinguish the three different Q ranges we give the Kratky plot as a the product $[I(Q)Q^2]$ in dependence on Q in an inset in Fig. 4. This representation divides out the Q^{-2} decay of the scattering, making other features more evident. Particularly, product $[I(Q)Q^2]$ in the Q range for the branching structure is now seen as constant, which is convenient for highlighting a logarithmic fractal structure of the tree images. In fact, the arrows pointing to the crossover points are needless in such a Kratky plot, though we added them for completeness. The slope between the arrows is equal to 0 ($\nu - 2 = 0.01 \pm 0.03$).

The part of the curve on the right side shows a feature deviating from the Q^{-2} decay in intensity in the range of large Q corresponding to 1–10 cm scales in the real space. We attribute this feature to the superposition of small different branches appearing upon projection of the real tree to the two-dimensional plane of the picture. This is especially true for small branches, since there are many of them on the tree. It is probable that the branching structure on the scale of 1–10 cm obeys the same area-preserving rule as the rest of the branching system on the scale of 0.1–10 m. Thus we classify this feature as another artifact of this methodology proposed to
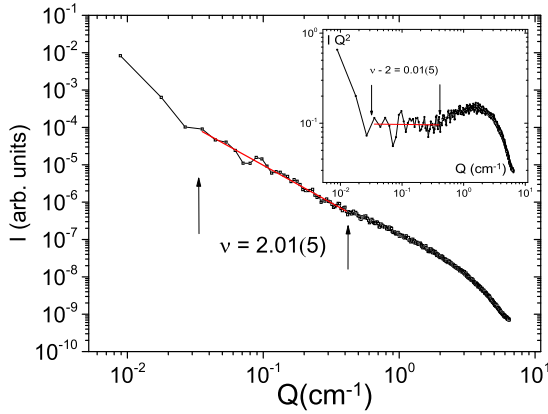
FIG. 6. Fourier intensity of the oak image as a function of the Fourier coordinate Q. The inset shows the Kratky plot $I Q^2$ as a function of Q.

study the tree structure. Another possibility is that change of the slope indicates the change of the structure for the young branches demanding that we separately consider the ranges of sizes for the old (growing for many years) branches from the young (growing for a year) ones. This question should be clarified by the comprehensive analysis of the tree image or by sophisticated selection of angles and scales when photographing the investigated tree.

We note that all curves taken from different images of various types of trees have the very same structure as shown in Fig. 4. Thus, a similar analysis applied to the image of an oak tree (Fig. 5) resulted in the curve shown in Fig. 6 that demonstrates clearly the presence of a range of momentum transfers where the function $I(Q)$ exhibits dependence described by Eq. (2) with $\nu = 2.01 \pm 0.05$. The spectral intensity shown in the manner of a Kratky plot is given as the inset of Fig. 6. It gives no dependence on Q ($\nu - 2 = 0.01 \pm 0.05$) in the corresponding Q range. We can assure the reader that similar analysis of the images applied to other trees, such as maple, chestnut, and linden (many different pictures), resulted in pictures, similar to Figs. 4 and 6, with the slope for branching system with ν close to 2.

Thus, we observe undeniable similarity of the curves representing the Fourier images of very different deciduous trees. It can be concluded that the branching structure of these trees is described by the class of logarithmic fractals. We show experimentally that indeed the trees obey the *Leonardo-like* rule upon their growth and year-by-year branching. We call this rule *Leonardo-like*, since it is applied not to the cross sections of a branch $\pi d^2/4$ but to its surface area $\pi d \, l$. Note that no trees were harmed during these experiments. The nondestructive method proposed can be used for an express analysis and scientific investigation of deciduous trees.

It is experimentally shown that the branching system of the real trees obeys in the Fourier space the scaling law proportional to Q^{-2}, which is equivalent to the logarithmic fractal structure of the object under study. The logarithmic fractal structure is equivalent to the area-preserving rule, but for the side view of a real tree, that is, the projection of the tree to the two-dimensional plane. In fact, we have

proven that the following area-preserving rule holds for the tree $d_i \, l_i = k \, d_{i+1} \, l_{i+1}$ in the range of sizes from 0.1 to 10 m. This experimental findings should either replace or supplement the Leonardo's rule $d_i^2 = k \, d_{i+1}^2$. Independent of whether Leonardo's rule is valid or not, the above presented experimental results show that the surface area of the cylinder-like branches equal to $\pi d_i l_i$ is equal to the sum of surfaces of the k cylinder-like branches of the next generation $k\pi d_{i+1} \, l_{i+1}$. In the other words, it is only the surface of the branches of the tree that matters. We can conclude that the life of a tree obeys the area-preserving laws of two-dimensional space. This conclusion allows one to distinguish between the growing part of the tree (surface) and already mature (internal) part, at least in models obeying the area-preserving rules.

V. CONCLUSION

In conclusion, we propose a method of studying tree structure with Fourier analysis of its image inspired by the small-angle (x-ray or neutron) scattering technique. The applied method can be used to show the logarithmic fractal structure of the branching system of deciduous trees. We have proven that the logarithmic fractal structure is equivalent to the area-preserving principle of the tree growth. Moreover, the experiments dealing with the side view of the tree complement Leonardo's principle with knowledge on the length of the branches but not exclusively on their thickness. We believe that this knowledge can help in building a correct mathematical model of real trees.

APPENDIX A

Let us consider the "Leonardo da Vinci" tree, which is based on the principle of equality of areas of different generations: the total area of elements added at each step is the same and equal to the area of the trunk, while each branch is split to four more branches so that at each step, four times more elements appear than at the previous generation (see an inset in Fig. 1). Since at each step the length of the side of the added squares is two times smaller than that at the previous step, the size of the square of the ith generation is equal to $r_i = A_0/2^{(i-1)}$, where A_0 is the linear size of the "trunk."

The generation number of the fractal n can be expressed via the size ratio of the largest and smallest elements of the tree:

$$n = \log_2 \frac{2A_0}{r_n}. \tag{A1}$$

Further, an area of each of the n generations is equal in area to the trunk and can be covered by exactly $2^{2(n-1)}$ minimal elements (squares) with area r_n^2. In total the tree is composed of n generations, and the entire tree of the nth generation is covered by $n \, 2^{2(n-1)}$ minimal squares. Knowing the area of the minimal square r_n^2, we can find the area of the entire tree

of the nth generation:

$$S_n = r_n^2 \, n \, 2^{2(n-1)}. \tag{A2}$$

We substitute the expression for $n(r_n)$ [Eq. (A1)] into Eq. (A2):

$$S_n = r_n^2 \, \log_2 \frac{2A_0}{r_n} \frac{A_0^2}{r_n^2} = A_0^2 \, \log_2 \frac{2A_0}{r_n}. \tag{A3}$$

Thus, when the area-preserving principle (Leonardo da Vinci rule) is fulfilled, then the total area of the tree grows logarithmically with a decrease in the minimal element of the fractal, that is, with an increase in the number of generations.

The measure of such an object as the Leonardo tree, according to Mandelbrot's definition [15], is

$$\mu(r) = h(r) N(r), \tag{A4}$$

where $N(r)$ is the number of squares of size r needed to cover the object. If $r \to 0$, and the measure $\mu(r)$ is finite $\mu(r) =$ const, then $h(r)$ is a probing function that defines the object as a fractal. The number of squares $N(r)$ of size r that can cover an infinite fractal is $S(r)/r^2$. Substituting Eq. (A3) into Eq. (A4) one finds

$$\mu(r) = h(r) A_0^2 \, r^{-2} \, \log_2 \frac{2A_0}{r} = \text{const}, \tag{A5}$$

whence the probing function $h(r)$ of this object is equal to

$$h(r) = r^2 \left(\log_2 \frac{2A_0}{r} \right)^{-1}. \tag{A6}$$

That is, the Leonardo tree is described by the probing function with a topological dimension of 2 and a logarithmic subdimension (-1), in accord with Mandelbrot's definition [16]. That means the Leonardo tree is a logarithmic fractal.

Let us now prove the statement in an opposite direction, that is, if we have a logarithmic fractal described by the Hausdorff measure of the form $\mu(r) = r^2 \, (\log_2 \frac{2A_0}{r})^{-1} N(r) =$ const, then such a fractal is constructed according to the area-preserving principle at each generation, that is, it is built in accord with the Leonardo's rule of the tree. Here it is called logarithmic, since the probing function contains a logarithm, and the fractal implies self-similarity in its move from one generation to another; in particular, the ratio of the linear sizes of elements of one generation to another remains constant.

Since $N(r)$ is the number of squares of size r needed to cover the fractal, the area of the entire fractal is equal to

$$S(r_n) = r^2 N(r) = \text{const} \log_2 \frac{2A_0}{r}. \tag{A7}$$

The difference in the areas of two successive generations of such fractal is equal to

$$\Delta S(n) = S(r_{n+1}) - S(r_n) = \text{const} \log_2 \frac{r_n}{r_{n+1}}. \tag{A8}$$

In the case of a fractal, the ratio of linear sizes for elements in two successive generations is constant and does not depend on the generation number:

$$\frac{r_n}{r_{n+1}} = \text{const}_1, \tag{A9}$$

so the area $\Delta S(n)$ added at each new generation will be constant and satisfy the Leonardo's principle of tree growth. Note that in the case of the tree, const$_1 = \sqrt{k}$, where k is the branching number. It can be shown that the constant in Eq. (A7) is equal to const $= 2A_0^2 / \log_2 k$, and if the number of branches is four, then const $= A_0^2$.

APPENDIX B

Let us derive the expression for the correlation function of the fractal objects in the two-dimensional space. By definition, the correlation function is a probability function describing how density of the object varies with distance. It is conveniently related to the scattering cross section via a Fourier transform.

1. *Case of logarithmic fractal.* The numerical experiments has shown that the logarithmic fractals and the picture of the Leonardo tree, as an example, give the scattering curves which are well described by Q^{-2} decay. Let us consider the logarithmic fractal with the finite size ξ; then the scattering intensity is given by Eq. (2) with $\nu = 2$, i.e., by the Lorentzian. The correlation function in this case can be calculated as

$$\begin{aligned}
\gamma(r) &\sim \frac{1}{2\pi} \int_{-\infty}^{\infty} \int_{-\infty}^{\infty} \frac{1}{1 + (Q\xi)^2} e^{iQ_x r_x + iQ_y r_y} dQ_x \, dQ_y \\
&= \frac{1}{2\pi} \int_0^{\infty} \int_0^{2\pi} \frac{Q}{1 + (Q\xi)^2} e^{iQr\cos(\phi)} d\phi \, dQ \\
&= \int_0^{\infty} \frac{Q}{1 + (Q\xi)^2} J_0(Qr) \, dQ = \frac{1}{\xi^2} K_0(r/\xi), \tag{B1}
\end{aligned}$$

where $J_0(Qr)$ is the Bessel function and $K_0(r/\xi)$ is the Macdonald function. Inside the fractal particle of a size ξ, i.e., in the approximation $r/\xi < 1$, the correlation function $\gamma(r)$ can be reduced to [28]

$$\gamma(r) \sim \ln(\xi/r). \tag{B2}$$

2. *General case.* Let us now derive the correlation function of the fractal object in the general case of two-dimensional space. The scattering function can be written as

$$I(Q) = \frac{C_\nu}{[1 + (Q\xi)]^{\nu/2}}, \tag{B3}$$

where ν varies from 1 to 3 and C_ν is a constant that depends on ν and is to be found by normalization of the correlation function. The correlation function of a fractal object is calculated via a Fourier transform of scattering intensity [Eq. (B3)]:

$$\begin{aligned}
\gamma(r) &= \frac{1}{2\pi} \int_{-\infty}^{\infty} \int_{-\infty}^{\infty} \frac{C_\nu}{[1 + (Q\xi)]^{\nu/2}} e^{iQ_x r_x + iQ_y r_y} \, dQ_x \, dQ_y \\
&= \frac{C_\nu}{2\pi} \int_0^{\infty} \int_0^{2\pi} \frac{Q}{[1 + (Q\xi)]^{\nu/2}} e^{iQr\cos(\phi)} d\phi \, dQ \\
&= C_\nu \int_0^{\infty} \frac{Q}{[1 + (Q\xi)]^{\nu/2}} J_0(Qr) \, dQ \\
&= \frac{C_\nu 2^{1-\nu/2}}{\xi^2 \Gamma(\nu/2)} (r/\xi)^{(\nu/2-1)} K_{\nu/2-1}(r/\xi). \tag{B4}
\end{aligned}$$

Constant C_ν is determined through the normalization of the correlation function:

$$\frac{C_\nu 2^{1-\nu/2}}{\xi^2 \Gamma(\nu/2)} \int_0^\infty (r/\xi)^{(\nu/2-1)} K_{\nu/2-1}(r/\xi) \, dr$$

$$= \frac{C_\nu 2^{1-\nu/2}}{\xi^2 \Gamma(\nu/2)} \xi \sqrt{\pi} 2^{\nu-1} \Gamma(\nu+1/2) = 1. \quad \text{(B5)}$$

Thus one obtains

$$C_\nu = \frac{\xi \Gamma(\nu/2)}{2^{\nu/2} \sqrt{\pi} \Gamma(\nu+1/2)} \quad \text{(B6)}$$

and expresses finally the normalized correlation function:

$$\gamma(r) = \frac{2^{1-\nu}}{\xi \sqrt{\pi} \Gamma(\nu+1/2)} (r/\xi)^{(\nu/2-1)} K_{\nu/2-1}(r/\xi). \quad \text{(B7)}$$

We note that Eq. (B7) can be simplified to Eq. (B1) in the case $\nu = 2$ that is reduced to Eq. (B2) in the small-r approximation, i.e., $r/\xi < 1$.

[1] J. P. Richter and R. C. Bell, *The Notebooks of Leonardo da Vinci* (Dover, New York, 1970).

[2] K. Shinozaki, K. Yoda K. Hozumi, and T. Kira, Jap. J. Ecol. **14**, 97 (1964).

[3] T. A. McMahon and R. E. Kronauer, J. Theor. Biol. **59**, 443 (1976).

[4] G. B. West, J. H. Brown, and B. J. Enquist, Science **276**, 122 (1997).

[5] G. B. West, J. H. Brown, and B. J. Enquist, Science **284**, 1677 (1999).

[6] G. B. West, B. J. Enquist, and J. H. Brown, Proc. Natl. Acad. Sci. USA **106**, 7040 (2009).

[7] F. Simini, T. Anfodillo, M. Carrer, J. R. Banavar, and A. Maritan, Proc. Natl. Acad. Sci. USA **107**, 7658 (2010).

[8] L. Koçillari, M. E. Olson, S. Suweis, R. P. Rocha, A. Lovison, F. Cardin, T. E. Dawson, A. Echeverría, A. Fajardo, S. Lechthaler *et al.*, Proc. Natl. Acad. Sci. USA **118**, e2100314118 (2021).

[9] R. Lehnebach, R. Beyer, V. Letort, and P. Heuret, Ann. Bot. **121**, 773 (2018).

[10] C. Eloy, Phys. Rev. Lett. **107**, 258101 (2011).

[11] R. Minamino and M. Tateno, PLoS ONE **9**, e93535 (2014).

[12] E. Nikinmaa, Acta Forestalia Fennica **235**, 7681 (1992).

[13] K. Sone, K. Noguchi, and I. Terashima, Tree Physiol. **25**, 39 (2005).

[14] K. Sone, A. A. Suzuki, S. Miyazawa, K. Noguchi, and T. Terashima, J. Plant Res. **122**, 41 (2009).

[15] B. Mandelbrot, *The Fractal Geometry of Nature* (Freeman, New York, 1983).

[16] J. O. Indekeu and G. Fleerackers, Physica A **261**, 294 (1998).

[17] L. Teia, Austral. Senior Math. J. **30**, 38 (2016).

[18] H. D. Bale and P. W. Schmidt, Phys. Rev. Lett. **53**, 596 (1984).

[19] P. Pfeifer and P. W. Schmidt, Phys. Rev. Lett. **60**, 1345 (1988).

[20] P.-Z. Wong and A. J. Bray, Phys. Rev. Lett. **59**, 1057 (1987).

[21] P.-Z. Wong and A. J. Bray, Phys. Rev. Lett. **60**, 1344 (1988).

[22] P.-Z. Wong and A. J. Bray, J. Appl. Crystallogr. **21**, 786 (1988).

[23] J. E. Martin and A. J. Hurd, J. Appl. Crystallogr. **20**, 61 (1987).

[24] J. Teixeira, J. Appl. Crystallogr. **21**, 781 (1988).

[25] E. G. Iashina and S. V. Grigoriev, J. Surf. Invest.: X-Ray Synchrotron Neutron Tech. **11**, 897 (2017).

[26] P. M. Pustovoit, E. G. Yashina, K. A. Pshenichnyi, and S. V. Grigoriev, J. Surf. Invest.: X-Ray Synchrotron Neutron Tech. **14**, 1232 (2020).

[27] https://github.com/tre3k/fractal.

[28] I. S. Gradshteyn and I. M. Ryzhik, *Table of Integrals, Series, and Products*, 7th ed. (Elsevier, New York, 2007), p. 919.